R. F. ACCELERATING STRUCTURES: THE CROSS-BAR STRUCTURE

A. Carne
Rutherford High Energy Laboratory, Chilton, England

1. Introduction

Interest in the Cross-Bar Structure is now centred on the energy range 100-200 MeV. Here it is being considered as an alternative to the Alvarez structure for the 200 MeV, 200 Mc/s, Pre-Injector Linac for the CERN 300 GeV A.G.S. project (1). The Cross Bar structure offers several advantages over the Alvarez Guide: Comparable shunt impedance, wide bandwidth and high group velocity in π-mode operation, physical compactness and good mechanical tolerances. In this energy range, focusing is a structure design requirement (though no specific calculations have been done so far), so that drift tube diameter must be chosen on the familiar basis of focusing, and r.f. breakdown capability in conflict with shunt impedance.

It is the purpose of this paper to report on the theoretical work, practical measurements on $\beta = .4$, $\beta = .56$ models, corresponding to 85 and 200 MeV, and further work on the early 400 Mc/s Cross-Bar Structure described elsewhere (2).

2. Theoretical

The major theoretical work is being carried out by Georges Dôme at CERN, and some of the conclusions are presented here.

The formation of field patterns has been derived on a basis of rectangular or square guide (where the side of the square equals the liner diameter), and the fields computed as if the currents were carried on the centres of the bars. Shunt impedance and Q at π-mode have been found as functions of bar diameter d_s and β, by assuming losses in the current carrying bars and side walls only. Losses in drift tubes and the non (total) current carrying bars are not included. If L, D, d, have meanings given in figure 8, and if $k = \omega/c$, $\ell = (D-d)/2$, we have

$$Q = Q_o \left\{ 1 + \frac{8}{\pi} \log\left(\frac{2L}{Kd_s}\right) \beta \left(\frac{\pi d_s}{4L}\right) F + \left(\frac{\pi d_s}{4L}\right) \frac{16 e^{-\pi D/L}}{1+2e^{-\pi D/L}} \right\}^{-1} \quad \ldots \text{ i)}$$

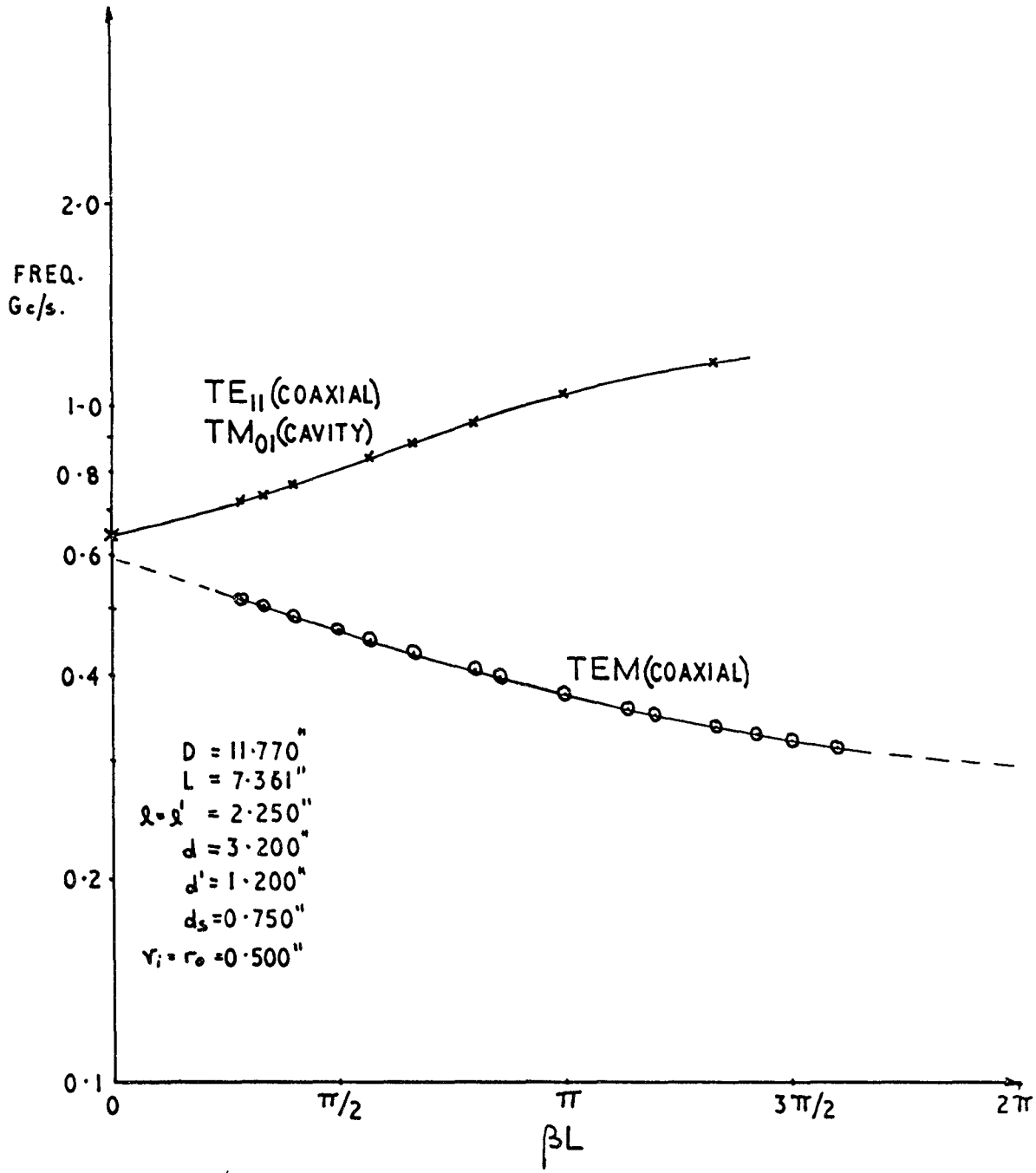

ω/β DIAGRAM FOR SYMMETRICAL CROSS-BAR

FIG. 1

where K is the complete elliptic integral: $K = \pi/2 \left(1 + 2e^{-\pi D/L} + \ldots\right)^2$;

$Q_o = \mathrm{Log}\left(\frac{2L}{Kd_s}\right) \frac{\pi d_s}{\lambda} \sqrt{\frac{\sigma}{\pi \epsilon f}}$ is the Q-value for losses on bars only ...

and $F = \pi/2 \left(k\ell + \sin k\ell \cos k\ell\right)^{-1} \geq 1$. Since D/L is usually >> 1,

$K \sim \pi/2$, and equation i) reduces to

$$Q \sim Q_o \left\{1 + \frac{8\beta}{\pi} \left(\frac{\pi d_s}{4L}\right) F \,\mathrm{Log}\left(\frac{4L}{\pi d_s}\right)\right\}^{-1} \quad \ldots \text{ iii)}$$

Equation iii) has been checked against the early 400 Mc/s model to give Q = 11, 200 against a measured 11, 900 (scaled from brass). This is very good agreement. Shunt impedance is given by:

$$\eta = \frac{QZ_o}{L} \frac{8M^2}{k\ell\,(1+\cot^2 k\ell) + \cot k\ell} = \frac{16}{\pi}\left(\frac{QZ_o}{L}\right)\left[M^2 F \sin^2 k\ell\right] \quad \ldots \text{ iv)}$$

where $Z_o = 60 \log\left(\frac{2L}{Kd_s}\right)$ is the characteristic impedance of a coaxial line, centre conductor d_s, (square) side L; and M is the transit time factor (the experimental approach to T. T. F. is given in section 4b). The variation of maximum shunt impedance with bar diameter and velocity is found by considering the maximum value of $(Q\,Z_o/L)$ with d_s and β. (The term inside the square bracket of eqn. iv) is proportional to (particle energy gain)^2/(stored energy), again discussed in section 4b). Considering only the second terms inside the bracket of eqn. i), we must maximise the function

$$\left(\frac{QZ_o}{L}\right) = \left(\frac{Q}{Q_o}\right)\frac{Q_o Z_o}{L} \propto \frac{\pi d_s}{4L} \frac{\left[\mathrm{Log}\left(\frac{\pi d_s}{4L}\right) - 2\,\mathrm{Log}\left(1+2e^{-\pi D/L}+\ldots\right)\right]^2}{1 + \frac{8}{\pi} F\beta\left(\frac{\pi d_s}{4L}\right)\mathrm{Log}\left(\frac{4L}{\pi d_s}\right)}$$

A good approximation to the maximum is given when

$$\mathrm{Log}\left(\frac{4L}{\pi d_s}\right) = 1 + \xi + \sqrt{1 + 0.541\gamma}$$

where $\xi = 2 \log\left(1 + 2e^{-\pi D/L} + \ldots\right) = 2 \log\left[1 + 2e^{-\frac{\pi D}{D-d}\left(\frac{2k\ell}{\pi}\right)\frac{1}{\beta}}\right]$, and

$\gamma = \frac{8}{\pi} F\beta$. Since ξ and γ increase with β, η decreases (slowly)

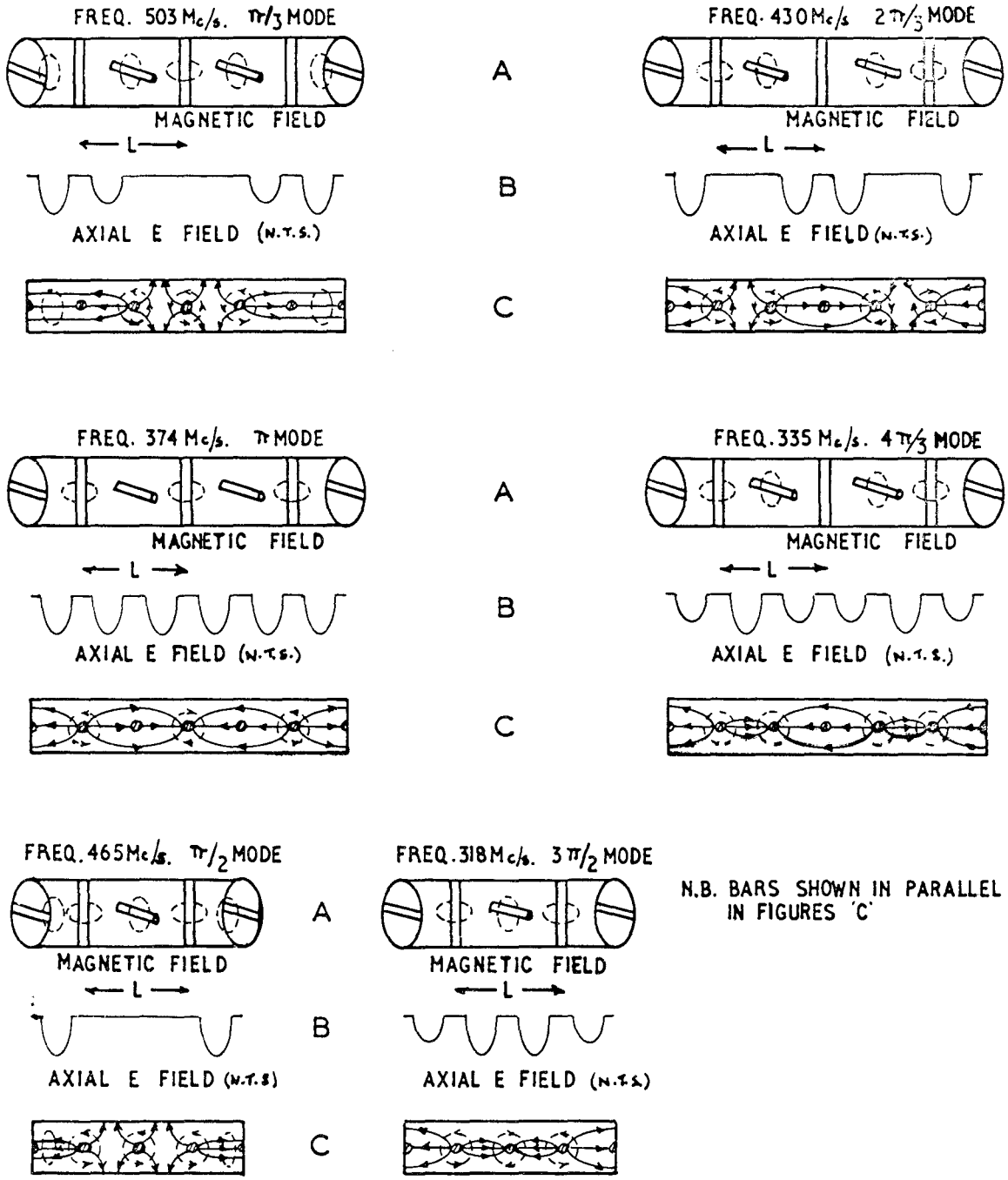

FIELD PATTERNS INSIDE CROSS-BAR STRUCTURE

FIG. 2

with β. If the optimum shunt impedance at $\beta = 0$ is given by unity, then we have for η and (L/d_s) opt:

β	(L/d_s) opt.	$\eta_{max.}$
0	5.8	1
.5	8.7	0.69
1	16.6	0.42

It is of interest to note that the bar need not be changed for $\beta = 0.5$ to 1.0. Over the energy range of interest (100-200 MeV), the fall of η max is 12%.

3. Field Patterns in the Cross-Bar Structure

Further measurements have been carried out on the early, symmetrical, 400 Mc/s model to determine field patterns in the various modes. This was done by axial field perturbation, and by magnetic loops through holes in the liner. The results are summarized in figures 1 and 2. In addition to the two $\omega - \beta$ branches shown in figure 1, there were many other resonances, all of them very much smaller than those plotted (of the order 30 db down) and may be H-modes, cable resonances, or harmonic resonances from the signal generator used.

The upper branch of the $\omega - \beta$ curve is obtained when the guide behaves as coupled coaxial resonators in the TE_{11} mode, giving rise to the TM_{01} mode along the guide. In this mode the magnetic field lines are purely circumferential, but distorted into oval, rather than circular, loops. Note also that for the TE_{11} mode (coax.) or TM_{01} guide, the zero mode can exist as the boundary conditions at the end plates can be satisfied. (The zero mode point in Figure 9, reference 2, is in fact the zero mode point for the upper branch). This mode has a forward fundamental, and is similar to the fundamental mode for the Alvarez structure. That this is so can be seen by linking together a series of coaxial resonators in the TE_{11} mode. Distorting the outside diameters to give a cylindrical waveguide with partitions reduces both 0 and π mode frequencies. Note the current flow is in opposite directions, 0-mode, and in the same direction in π-mode on either side of a partition. Cutting slots in the outside edges of the partitions in the direction perpendicular to the plane of the bars, does not affect the current lines in 0-mode, but shortens them in π-mode, i.e. causes the π-mode frequency to increase. The same effect can be seen by considering the capacitive effect of the slots. Putting in drift tubes loads down the two frequencies by roughly the same amount.

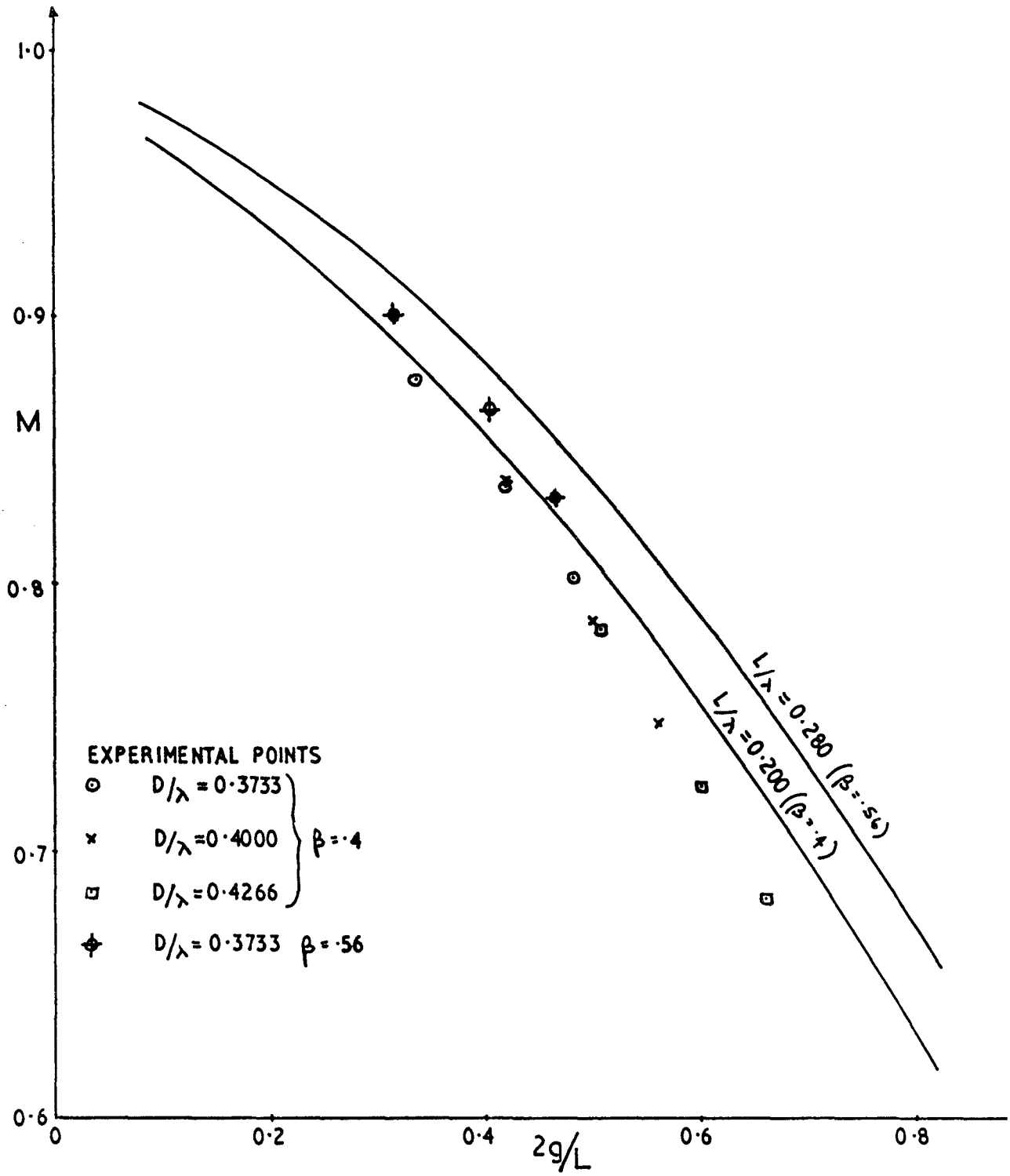

TRANSIT TIME vs. 2g/L IN CROSS BAR MODELS

FIG. 3

The "Cross-Bar Mode" is the lower branch in the $\omega - \beta$ diagram, and has been previously (2) described in terms of coupled coaxial resonators in the TEM (fundamental) mode*. (It should be remarked that this synthesis of modes in terms of partitioned coaxial resonators, rather than by starting with cylindrical guide with thin partitions, is preferable since it does allow for the effect of the finite thickness of the structure components). As such it is not possible to terminate the structure in 0 or 2 π (i.e. when all the bars act as coaxial resonators) modes. On the 4 whole section model used with terminations in half bars, in π -mode the magnetic field was seen to exist in loops round one set of bars, and none at all in the second set containing the terminations. Figure 2 shows the magnetic field patterns, and the axial field plots (N. T. S.) in some of the modes measured in the model. It can be seen that for modes $\theta < \pi$, circumferential as well as coaxial H fields can exist. How much the circumferential components of H fields depend on the terminations than perhaps on some hybrid coaxial mode is not clear at present. Further measurements on the model with flat-plate terminations are to be done to clarify this (and, more important to enable us to find the characteristics of the structure with one set of bars removed). For modes $2\pi > \theta \geq \pi$ H-lines coaxial with the bars only were found. In this short symmetrical model no degeneracy was seen (but not surprisingly). A long 30-cell model, without drift tubes, with bars whose diameters are in the ratio 2:1, has been made to study the π -mode region, but there are no results to report as yet. Although there is a physical asymmetry in a long structure, it should be possible to have a continuous $\omega - \beta$ curve at π mode and hence a high group velocity. For small gaps with resulting uniform E fields, asymmetries in the drift tube lengths will have only a second order effect on capacitance, referred to one set of drift tubes or the other. Equalizing the bar diameters (or nearly so) to give the same π -mode resonant frequencies has only a small effect on the shunt impedance. Fine tuning can be obtained by use of tuners in the neighbourhood of one set of bars.

---

*NB. In Yale Conference Report P121, figure 9A '0' -mode, ALL E-lines should go from bars to liner, and not only alternate bars as drawn.

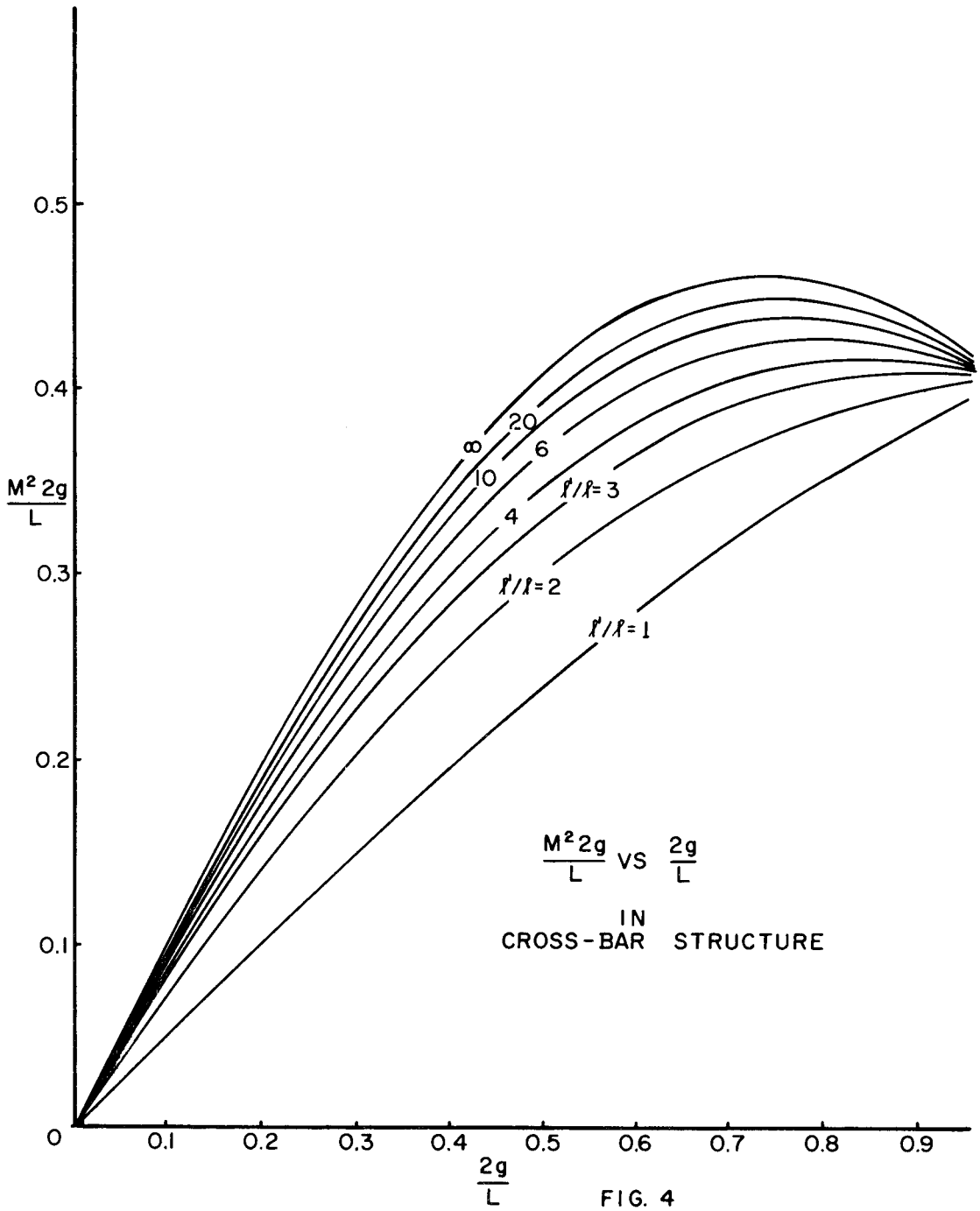
0.5
0.4
0.3
0.2
0.1
0
M² 2g / L
∞
20
10
6
4
ℓ'/ℓ = 3
ℓ'/ℓ = 2
ℓ'/ℓ = 1
M² 2g / L VS 2g / L
IN
CROSS-BAR STRUCTURE
0.1
0.2
0.3
0.4
0.5
0.6
0.7
0.8
0.9
2g / L

FIG. 4

4. Quarter-Scale Models for CERN 200 MeV Linac

Two 800 Mc/s (1+2 (1/2)) cell models have been made, for velocities $\beta = .4$ ($\sim$ 85 MeV) and $\beta = .56$ ($\sim$ 200 MeV). The two sets of drift tubes are of different lengths but constant diameters $d/\lambda = 0.0868$, corresponding to d = 5.125 inches, full scale, to enable them to house quadrupoles; drift tube bores $d'/\lambda = 0.0233$, as the value taken for the stage 1 design for the Alvarez structure. In each model, 3 different diameters for the current carrying bars (corresponding to L/d_s = 6, 8, 10) and 3 values of liner diameter ($D/\lambda = 0.373, 0.4, 0.427$, i.e. 14, 15, 16 cm at 800 Mc/s) were used. For a given liner diameter, for each diameter bar, the length of the 'large' drift tubes was adjusted to give a π-mode resonant frequency within 2 Mc/s of 800 Mc/s, and the η/Q measured. The liner was then bored out and the measurements repeated. The same sets of drift tubes and bars could be used, since boring out the liner increases the cavity inductance, and reducing the lengths of drift tubes (i.e. increasing gap lengths) reduces the capacitance and restores the resonant frequency. Bandwidths, defined here by $(f_{2\pi} - f_o)/f_\pi$ cannot be measured directly for the reasons given previously, but extrapolation from the modes measured give values of the order of 100%.

Further aspects of these models are discussed under separate headings..

(a) R.F. Breakdown

As yet there is no detailed information on the field distribution across the drift tubes, so that r.f. breakdown capabilities are not known. To this end, high power measurements are to be carried out in the near future. However, rough estimates on performance can be obtained from data given by Wilkins (3) for re-entrant cavities. Treating each half-cell as a separate cavity, for which T.T.F. (measured) and E_o (the mean gap field, assumed uniform) are known, then for the drift tubes for the given diameter and profiles given by $r_o/\lambda = 0.0127$, $r_1/\lambda = 0.0062$, (i.e. the same as the Rutherford Lab. or CERN 50 MeV Linacs), values of E_s/E_o in the range 1.2 - 1.5 for $\beta = .4$ - .56 can be expected, and for $E_s \gtrsim 14.7$ Mv/m (Kilpatrick's Criterion at 200 Mc/s) acceleration rates of the order 4 MeV/m could be achieved. Alternatively, and subject to the practical requirements of quadrupole focusing, smaller drift tube diameters could be used with a lower acceleration rate, with an improvement in shunt impedance. (Maximum shunt impedance requires that d/L and ℓ/d be as small as possible for a given (g/d), where the terms have the meanings given in figure 8).

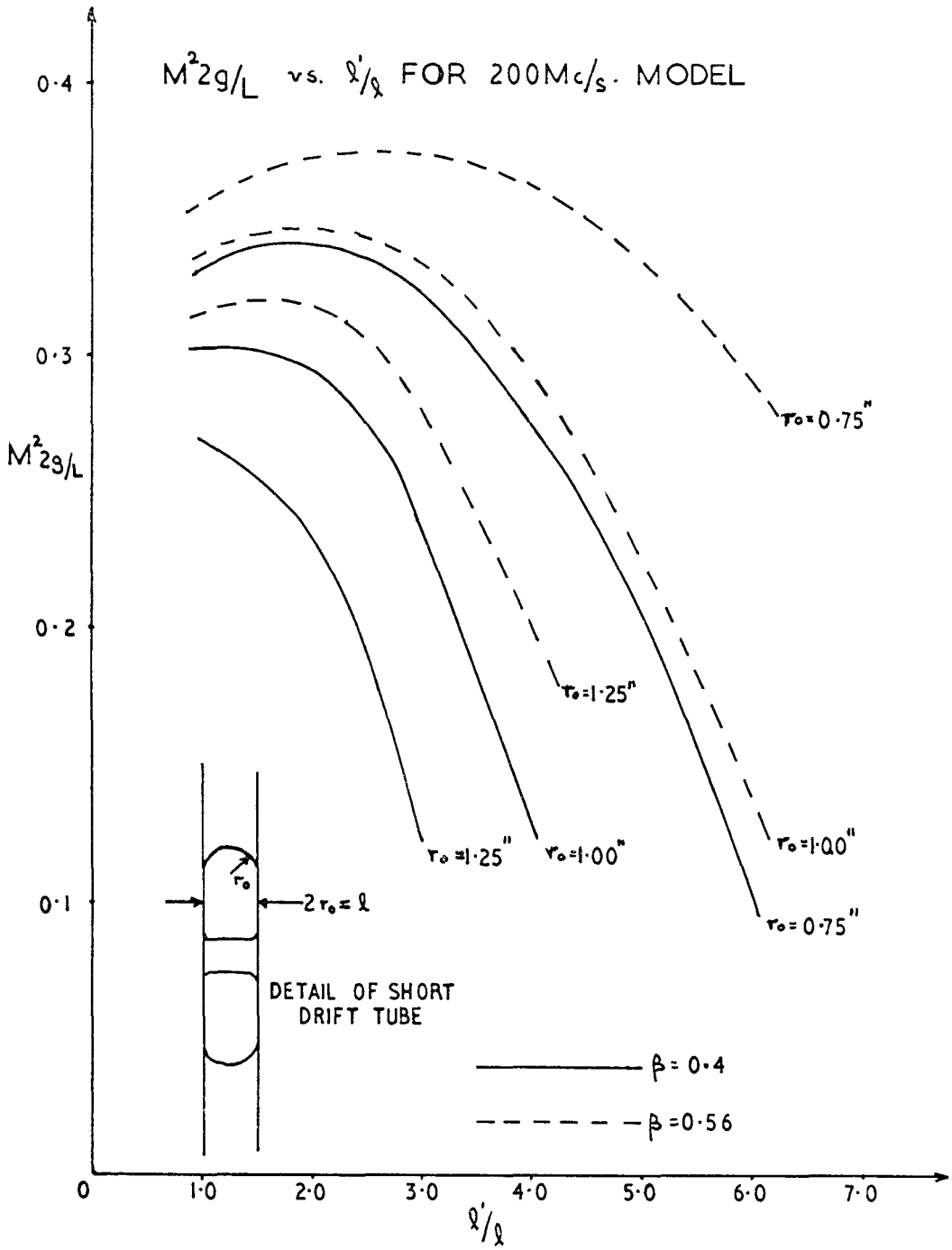
M²2g/L vs. l'/l FOR 200Mc/s. MODEL
0·4
0·3
0·2
0·1
0
M²2g/L
1·0
2·0
3·0
4·0
5·0
6·0
7·0
l'/l
r₀=0·75"
r₀=1·25"
r₀=1·00"
r₀=1·25"
r₀=1·00"
r₀=0·75"
r₀
2r₀=l
DETAIL OF SHORT DRIFT TUBE
β=0·4
β=0·56

FIG. 5

(b) Transit Time Factor, and η/Q

It was clear from the measurements on the early 400 Mc/s model that although the shunt impedance was high, so too was the content of higher order space harmonics. Since these contribute only to the losses, and not to acceleration, the Cross-Bar Structure is from this point of view still somewhat inefficient. By changing the lengths of drift tubes, but keeping the gap lengths constant so that the effect on resonant frequency is only second order, a change in harmonic content can be obtained. The π -mode wave form is given in the sketch, where

ℓ is the length of the small drift tube
ℓ' is the length of the large drift tube
L, periodic length, $= \ell+\ell'+2g$;
$\beta_o L = \pi$ for π -mode

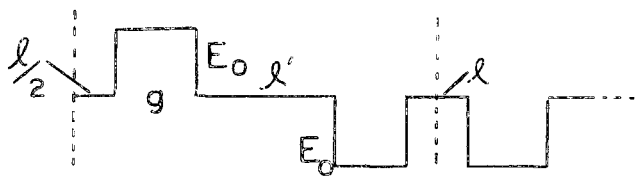

The field is assumed uniform in the region of the gaps (a fair assumption providing the gaps are small), and zero inside the drift tubes ℓ, ℓ'. The amplitude of the n^{th} harmonic is given by

$$(T.T.F.)_n = \int_0^L E(z)\cos\beta_n z\, dz \Big/ \int_0^L E(z)\, dz$$

$$= \frac{\sin\left(\frac{\beta_n g}{2}\right)}{\frac{\beta_n g}{2}} \sin\left(\frac{\beta_n L}{2}\right) \sin\frac{\beta_n}{2}\left(g+\ell'\right),$$

and for the fundamental, the T. T. F. is

$$M = \sin\frac{\pi g}{2L} \sin\frac{\pi}{2L}(g+\ell') \Big/ \pi g/2L .$$

Clearly the smaller the gap, the larger the T. T. F. (practically obtainable by use of small diameter drift tubes), and the smaller the drift tube ℓ,

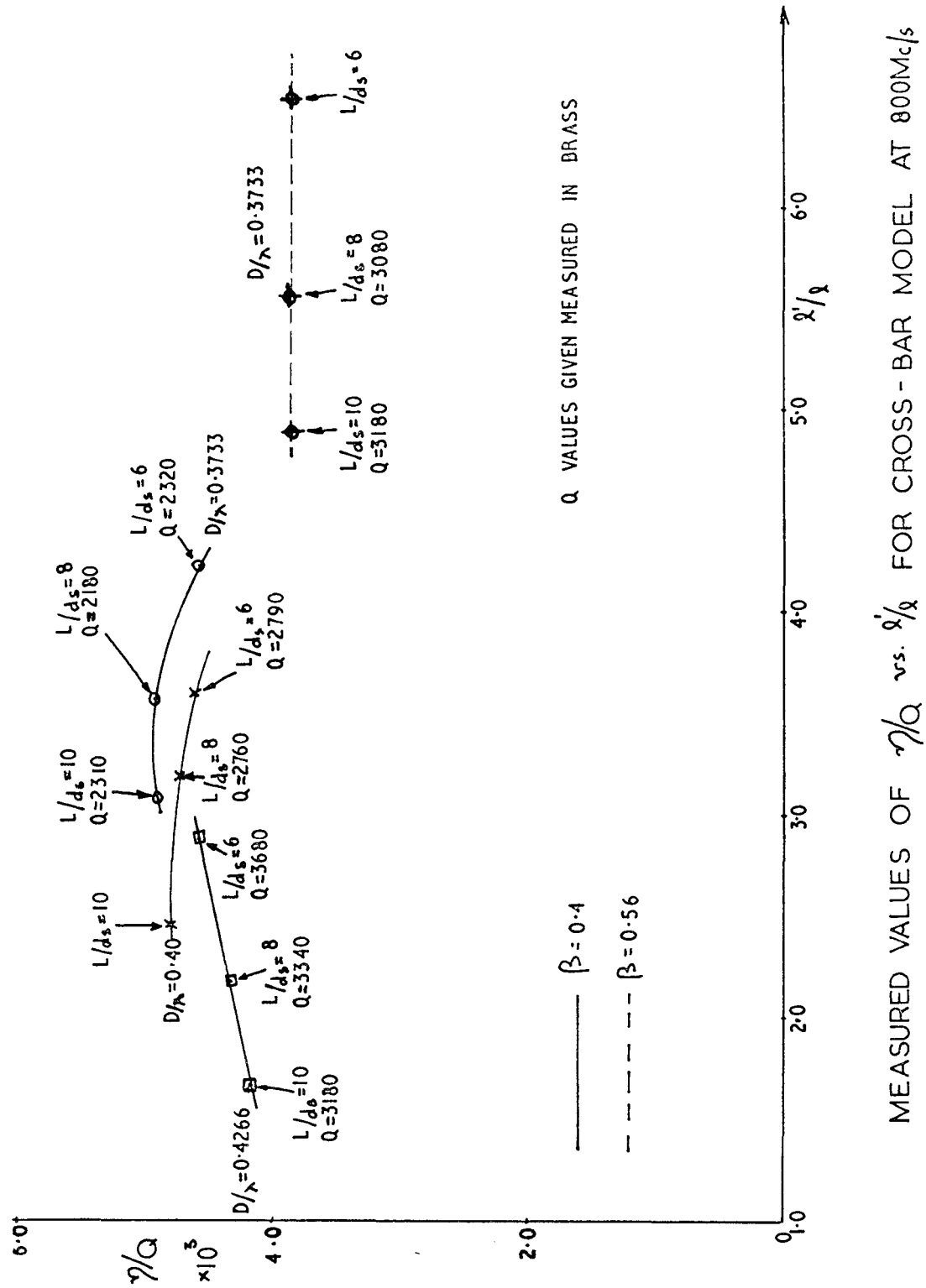

MEASURED VALUES OF η/Q vs. l'/l FOR CROSS-BAR MODEL AT 800Mc/s

FIG. 6

the greater the T. T. F.. Curves of T. T. F. to include the drift tubes geometries of the two models are given in figure 3, and compared with measured values: agreement is good for small gaps, $\sim 3/4\%$, but for larger gaps the error is larger, $\sim 5\text{-}1/2\%$, as to be expected since the gap field becomes non-uniform (but more like $1/r$ variation from the large drift tubes, as for a coaxial field).

The optimum efficiency for the structure is when the ratio (Energy gain per unit length)^2/(Stored energy per unit length) is a maximum, i.e. the stored energy needed to produce a required accelerating field in a minimum. This ratio is proportional to η/Q, and for small gaps, proportional to $M^2(2g/L)$. Curves of $M^2(2g/L)$ against $(2g/L)$ for values of ℓ'/ℓ are plotted in figure 4. For most values of ℓ'/ℓ the optimum ratios are for $(2g/L) \sim 0.7\text{-}0.8$. Note that the maximum value is for $\ell'/\ell = \infty$, i.e. when there are no small drift tubes, and $(2g/L) = 0.74$, but since field lines exist round these bars and drift tubes in the $(\pi, 2\pi)$ region, doing this removes some capacitive loading, with a consequent reduction in bandwidth. For ℓ'/ℓ 3-4 there is little variation in $M^2(2g/L)$ with $(2g/L)$ in the range 0.6-0.8. For a given small drift tube length ℓ (as used in both models where ℓ = stem diam. = 2 x outer profile radius, equal to 1-1/2 inches at 200 Mc/s) $M^2(2g/L)$ is given in figure 5, where the optimum values are for $\ell'/\ell \sim 2$, $\beta = .4$; $\ell'/\ell \sim 3$, $\beta = .56$.

For a given liner diameter, for each value of bar diameter, the large drift tubes were machined to give the correct frequency, and the (η/Q) value was measured, according to the formula

$$\eta/Q = A \left(\int_0^L E(z) \cos \beta_n z \, dz \right)^2 / \omega \epsilon L, \quad \beta_n = \beta_0 = \pi/L$$

where ϵ is the stored energy, and A = 2 for T. W. operation, = 1 for S. W. (e.g. π). (Results given previously (2) were in fact for T. W. operation, so that π-mode values should be reduced by a factor 2). Results obtained so far are given in figure 6, and scaled to 200 Mc/s ($\eta/Q \propto 1/\lambda$), in table 1 below. Values of η/Q are between 2 (at $\beta = .4$) and 3 ($\beta = .56$) times greater than corresponding values for the Alvarez structure (1). That there is a change of shape in the sets of points ($\beta = .4$) is in agreement with figure 5, where for D = 14, 15 cm (model) all points are to one side of the peak, but for D = 16 cm. includes the peak.

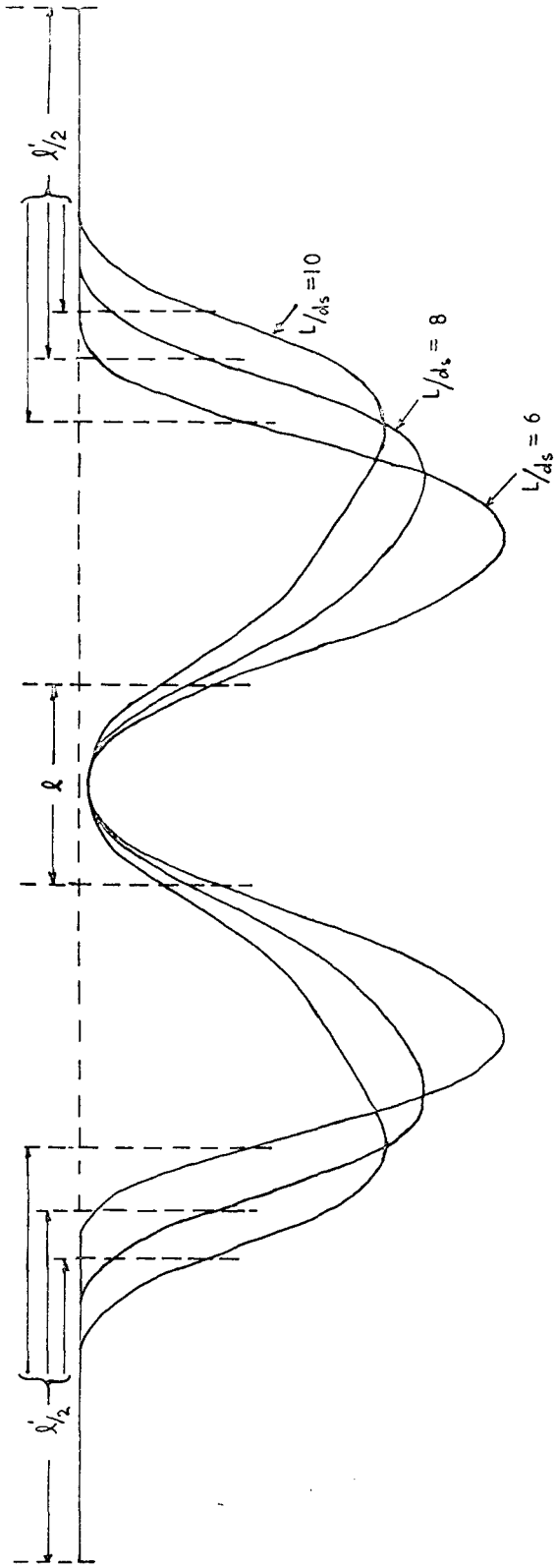

FIG. 7 PLOT OF $\Delta f \propto |E|^2$ AT $\beta = 0.4$ (D=14cm)

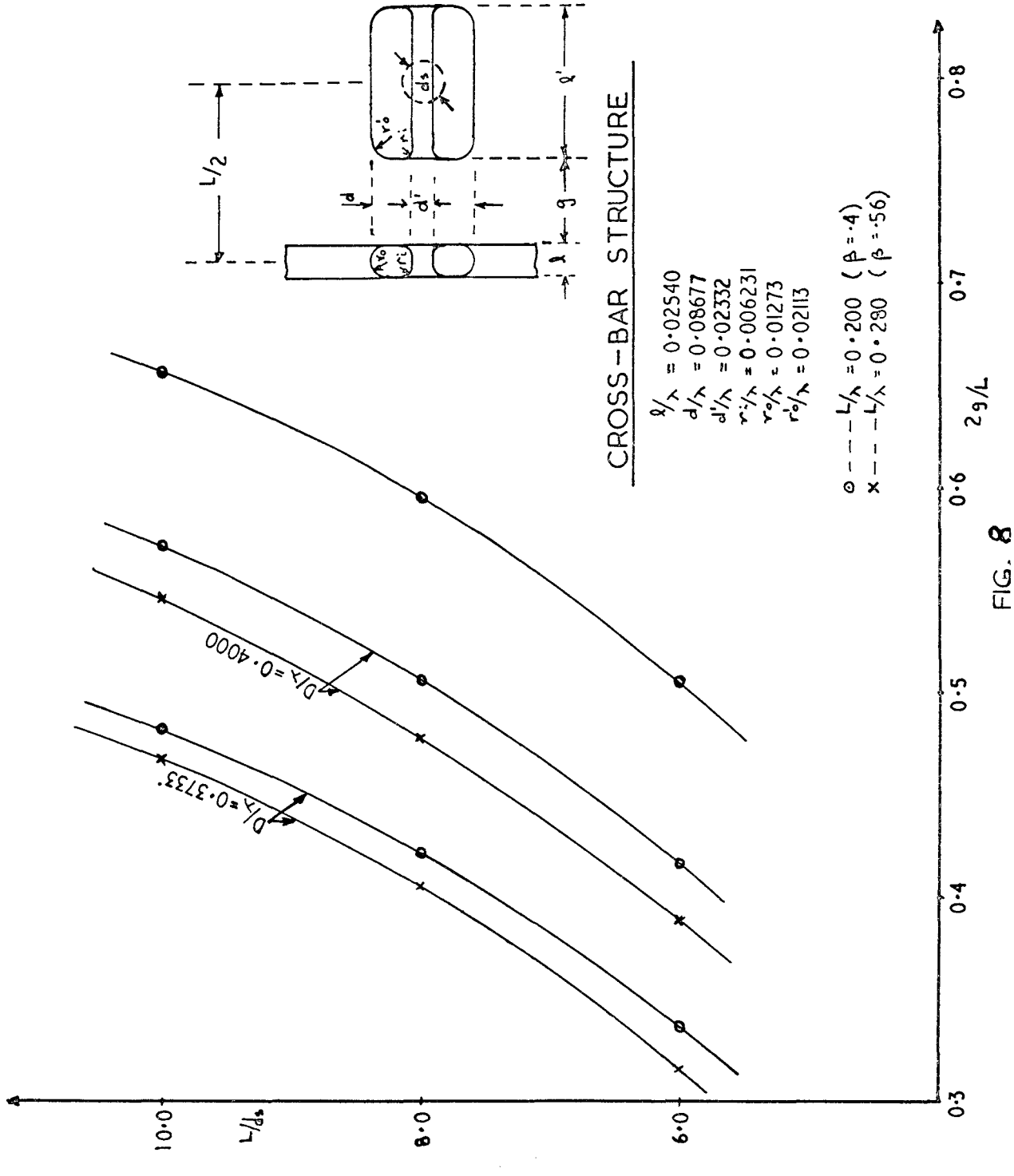
CROSS-BAR STRUCTURE
ℓ/λ = 0·02540
d/λ = 0·08677
d'/λ = 0·02332
r₁/λ = 0·006231
r₂/λ = 0·01273
r'₀/λ = 0·02113
○ — — L/λ = 0·200 (β = ·4)
× — — L/λ = 0·280 (β = ·56)
L/2
d
d'
g
g'
ℓ'
D/λ = 0·4000
D/λ = 0·3733
L/d_s
10·0
8·0
6·0
0·3
0·4
0·5
0·6
0·7
0·8
2g/L

FIG. 8

TABLE 1

800 Mc/s CROSS BAR MODEL MEASUREMENTS

$\beta = 0.4$ $\ell = 0.375''$

D (cm)	L/d_s	2g/L	ℓ'/ℓ	M	M(cal)	η/Q	Q (Brass)	η/Q (Scaled to 200 Mc/s)	η/Q th. 800 Mc/s
14	6	0.337	4.219	0.8757	0.8845	4.55×10^3	2,320	1.14×10^3	4.50×10^3
14	8	0.421	3.560	0.8371	0.8472	4.91×10^3	2,180	1.23×10^3	4.72×10^3
14	10	0.482	3.080	0.8026	0.8178	4.87×10^3	2,130	1.22×10^3	4.83×10^3
15	6	0.417	3.592	0.8390	0.8486	4.58×10^3	2,790	1.15×10^3	
15	8	0.501	2.931	0.7866	0.8080	4.68×10^3	2,760	1.18×10^3	
15	10	0.561	2.453	0.7481	0.7764	4.78×10^3	-	1.20×10^3	
16	6	0.507	2.880	0.7821	0.8050	4.55×10^3	3,680	1.14×10^3	
16	8	0.597	2.176	0.7246	0.7565	4.30×10^3	3,340	1.07×10^3	
16	10	0.661	1.666	0.6816	0.7195	4.16×10^3	3,180	1.04×10^3	
$\beta = 0.56$		$\ell = 0.375$							
14	6	0.317	6.533	0.9008	0.9155	3.83×10^3	-	0.96×10^3	
14	8	0.405	5.560	0.8652	0.8808	3.86×10^3	3,080	0.97×10^3	
14	10	0.466	4.885	0.8315	0.8537	3.82×10^3	3,180	0.96×10^3	
15	6	0.388	5.747				3,610		
15	8	0.479	4.739				3,630		
15	10	0.543	4.035				3,290		

Proceedings of the 1964 Linear Accelerator Conference, Madison, Wisconsin, USA

Of particular interest is the set of perturbation curves shown in figure 7, for the $\beta = .4$, D = 14 cm model. The distorting effect on gap field of increasing gap length can be seen. Comparison of the $L/d_s = 6$ and 10 curves shows that for $L/d_s = 6$, η/Q is 7% greater and the peak total E-field 18% LESS than for $L/d_s = 10$. Generally as the gap increases (i.e. ℓ' gets smaller), the peak total E-field decreases, but not necessarily (η/Q).

Q values on the models are also included in figure 6 and the table, showing generally that as the volume of the cavity is increased (increasing D for a given L, or vice versa) Q increases, and for a given model, Q increases more rapidly than (η/Q) decreases with D. For a given D and L, Q decreases slowly with increasing L/d_s. The actual Q values are low due to the multiplicity of dry (demountable) joints: in particular the joints of the current carrying bars with liner used indium rings in grooves in the liner. (Since these joints will carry a heavy current in high power conditions, their quality becomes a major problem). The final 800 Mc/s model will have soldered joints to give a more representative Q-value. Scaled to 200 Mc/s and copper, the model values become of the order 12-14000. At least a doubling of this value is hoped for in the high power structure with good joints.

(c) Dimensional Tolerances

As already stated, for given D, d_s the large drift tubes ℓ' were machined to give the correct frequency. A summary of dimensions for constant frequency in the models is given in figure 8. From the data obtained we deduce the following tolerances per thousandth inch

	$\beta = .4$	200 Mc/s	$\beta = .56$
D	7 kc/s		7.3 kc/s
bar d_s	25 kc/s		21 kc/s
ℓ' (or total gap)	11 kc/s		8.75 kc/s

These tolerances are generally very similar to the Alvarez structure at 200 Mc/s and can be seen to get easier with increasing energy.

5. Conclusions

Model measurements show the Cross-Bar Structure to have (η/Q) values between 2 and 3 times greater than the Alvarez Structure in the range 100-200 MeV. Providing the theoretical Q-values can be achieved - and this requires attention to r.f. joints, particularly between the current carrying bars and line - then the Cross-Bar Structure should have shunt impedances

(200 Mc/s, $\phi_s = 0$) of the order 25-20 M Ω/m between 80-100 and 200 MeV. These values are comparable with the Alvarez structure at 80-100 MeV, and certainly better at 200 MeV. (At much higher energies ($\beta \sim 1$), the shunt impedance would be of the order 30%-50% less than the values quoted (i.e. $\sim$ 25 M Ω/m at v = 0, 800 Mc/s).) Further enhancement of these figures can be achieved by increasing D and reducing d, ℓ to obtain ratios nearer (2 g/L) $\sim$. 7, (ℓ'/ℓ) $\sim$ 3 - 4, giving optimum values for M^2 (2 g/L). Reduction of ℓ, d now depends on requirements for focusing, and r.f. breakdown capabilities. Future work will include high power model measurements to assess the r.f. voltage breakdown performance, and to check the design of r.f. joints.

Further advantages of the Cross-Bar Structure are its physical size (where the liner diameter is now of the order 60 cm, compared with the $\sim$80 cm Alvarez guide at β = .4), its mechanical tolerances (certainly no worse than the Alvarez guide), and its high group velocity v_g. If the structure is symmetrical, then at π-mode $v_g \neq 0$ (and on the early 400 Mc/s model v_g = 0.193 c); if the structure is asymmetric (as is required by transit time considerations above), a continuous $\omega - \beta$ curve at π-mode is still possible by selective tuning. Again, future work will include a study of the region around π-mode to determine the magnitude of mode splitting in an asymmetric structure and the effects of correction.

6. Acknowledgments

The author would like to express his thanks to Dr. George Dôme of CERN for making freely available his theory of the Cross-Bar Structure, and for much stimulating discussion, and Mr. Normal Fewell who carried out the experimental measurements.

NAGLE: Did you say your practical value for shunt impedance was 20 megohms per meter?

CARNE: Yes, 20 megohms per meter at 200 MeV and 200 Mc is a value that we expect to achieve. This includes all losses.

KNAPP: How did you scale that result?

CARNE: Taking the Q values that we have in the 800 Mc model, Q's of around 3000 to 3500, and scale from brass to copper, and from 800 to 200 Mc, we get Q's of about 14,000. Experience suggests that we can increase this value by a factor 1-1/2, by making the models with better joints. An important point about these model measurements is that the cavities were demountable in many ways in order to change the outside

diameter, stem diameter and drift tube length. In particular, the cross section of the joint of a current-carrying bar with the liner is shown in the sketch. Contact was made by compressing indium rings in grooves in the body of the liner. (Three grooves were cut: one for each of the three liner diameters, D, used). It was hoped that this system would give good rf contact, but, in fact, it turned out to be rather poor. This is similar to the experience that we also had on the original 400 Mc/s model (described at the Yale Conference). There we had dry joints, and the Q's were poor. As we increased the number of cells, instead of the Q increasing as expected, we found it actually went down due to the increase in number of joints. We have really to make good soldered rf joints to get good Q values.

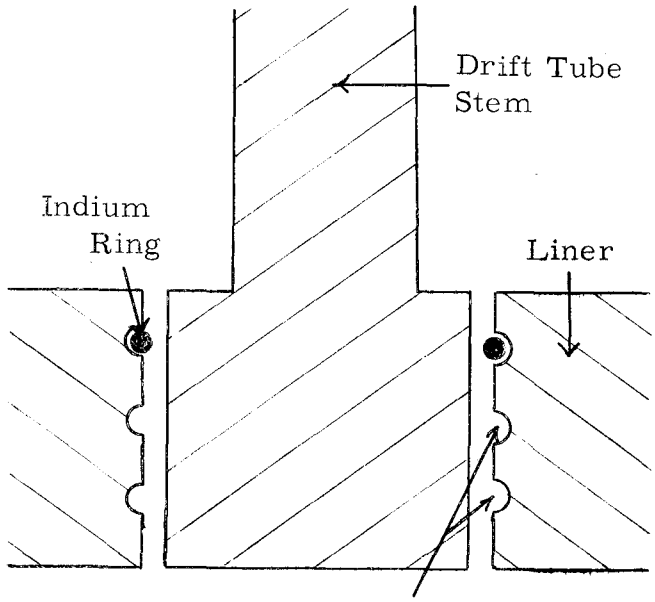

HUBBARD: How many cells are there in your model?

CARNE: On the 800 Mc models we have one full cell and two half cells for doing the R/Q measurements. We are not taking end plate losses into account for the Q values, it not being necessary in the cross-bar structure.

GIORDANO: As you increased the drift tube diameter, you found an increase in shunt impedance and a decrease in field intensity. Was this decrease in field intensity on the axis? And were there any other regions where the field was higher?

CARNE: That I don't know. The actual plot you saw was just that of an axial field perturbation.

References

(1) "Design of a High Current 200 MeV Proton Linear Accelerator".

A Carne, K. Batchelor, NIRL/R/55 March 1964, and Yale Linac Conference Report, p 404, October 1963.

(2) "Structures for High Energy Proton Linear Accelerators". A Carne.

International Conference, Dubna, August 1963; also Yale Conference, October 1963.

(3) "Design Notes on Resonators for P.L.A.'s" J. J. Wilkins. AERE GP/R 1613, 1955.